

A Deep Learning Approach to Grasping the Invisible

Yang Yang¹, Hengyue Liang² and Changhyun Choi²

Abstract—We introduce a new problem named “grasping the invisible”, where a robot is tasked to grasp an initially invisible target object via a sequence of non-prehensile (e.g., pushing) and prehensile (e.g., grasping) actions. In this problem, non-prehensile actions are needed to search for the target and rearrange cluttered objects around it. We propose to solve the problem by formulating a deep reinforcement learning approach in an actor-critic format. A critic that maps both the visual observations and the target information to expected rewards of actions is learned via deep Q-learning for instance pushing and grasping. Two actors are proposed to take in the critic predictions and the domain knowledge for two subtasks: a Bayesian-based actor accounting for past experience performs explorational pushing to search for the target; once the target is found, a classifier-based actor coordinates the target-oriented pushing and grasping to grasp the target in clutter. The model is entirely self-supervised through the robot-environment interactions. Our system achieves 93% and 87% task success rate on the two subtasks in simulation and 85% task success rate in real robot experiments, which outperforms several baselines by large margins. Supplementary material is available at: <https://sites.google.com/umn.edu/grasping-invisible>.

Index Terms—Dexterous Manipulation, Deep Learning in Robotics and Automation, Computer Vision for Automation

I. INTRODUCTION

Imagine what happens when a young kid is looking for a specific toy block buried in clutter, as shown in Fig. 1a. He or she may first push down the pile of the blocks and luckily spot the target block in clutter, then push around it to make a space for the fingers (we refer to this type of motion as “singulation” [1]) and finally grasp it. We have wondered if an intelligent agent can perform such a task. Can the robot search for an invisible target object to make it visible, then singulate the target by pushes to facilitate grasping? This requires the robot to have the ability of explorational pushing, singulation by instance pushing (i.e., push the target or surrounding objects to free the space around the target instance) and instance grasping, in order to grasp the invisible target.

Robot pushing [1], grasping [2] or push-grasping [3] has been actively studied but mostly target-agnostic. Without incorporating target information effectively, fast adaptations (e.g., by applying the target mask) of these methods for target-oriented tasks are not successful. While some target-oriented manipulations [4], [5] have been applied to the



(a) Configuration

(b) Our approach

Fig. 1: **Example configuration of the “grasping the invisible” problem.** The target object is the green cylinder and initially invisible to the robot. We propose to solve the problem by the exploration-singulation-grasping procedure.

clearly visible target in sparse environments (i.e., the target is placed well isolated), the type of scenes where target-oriented manipulations could be applied are limited.

Moving forward from target-agnostic robotic manipulations to target-oriented manipulations brings challenges to not only the perception system but also the manipulation capabilities. Specifically these challenges are: 1) target information is missing in the case of complete occlusion and efficient exploration is required, 2) perception modules responsible for reasoning about the target region tend to work poorly in dense clutter, 3) data labeling in target-oriented tasks is too expensive and 4) the coordination between pushing and grasping (i.e., deciding when and how to push or grasp) is critical but tricky to accomplish.

In this paper, we propose to solve the “grasping the invisible” problem by formulating a deep learning approach in an actor-critic format. The key aspects of our system are

- A robust semantic segmentation module is used to annotate the objects of interest and detect the existence of the target.
- We learn a deep Q critic with a fully convolutional network (FCN) that takes visual observations and the target mask as input and predicts expected rewards (i.e., Q values) for potential instance pushing and grasping as output.
- By incorporating Q predictions with domain knowledge, two actors are proposed to make pushing or grasping action in different scenarios. Specifically, a Bayesian-based actor accounting for past experience performs efficient explorational pushing in the complete occlusion. Once the target is visible, coordinated decision making in instance pushing or grasping is achieved by a classifier-based actor which takes the clutteredness around the target as an input.
- Our learning models (the critic and the coordination actor) are fully self-supervised through the robot-

*This work was in part supported by the MnDRIVE Initiative on Robotics, Sensors, and Advanced Manufacturing.

¹Y. Yang is with the Department of Computer Science and Engineering, Univ. of Minnesota, Minneapolis, USA yang5276@umn.edu

²H. Liang and C. Choi are with the Department of Electrical and Computer Engineering, Univ. of Minnesota, Minneapolis, USA {liang656, cchoi}@umn.edu

environment interactions.

Fig. 1 presents an example configuration of the “grasping the invisible” problem and how we propose to solve it.

Contributions To our best knowledge, this is the first work that studies the “grasping the invisible” problem in robotic manipulation. This paper presents two core technical contributions: 1) a critic for instance pushing and grasping learned by deep reinforcement learning and 2) a Bayesian-based actor for target exploration and a classifier-based actor for grasping in clutter. Our system can perform target-oriented manipulation tasks with observations from an RGB-D camera.

II. RELATED WORK

Robotic grasping has been well studied and shown great success. Classic model-driven approaches [6], [7] find stable force closures for known objects grasping by utilizing prior knowledge such as 3D models of manipulators and objects and their physical properties. More recent data-driven approaches [8], [9], [2] harness learning algorithms and data (collected from humans or physical experiments) to directly map visual observations to grasp representations. Our approach is data-driven and model-agnostic, and the learning models are trained by self-supervision.

To mitigate uncertainty and collision introduced by clutter, non-prehensile manipulations [10], such as pushing, are investigated in both model-driven approaches [11], [12], [13] and data-driven approaches [1], [14], [15]. With the addition of pushing, push-grasping systems [16], [3] are advanced. Analogous to these methods, our approach learns non-prehensile pushing to facilitate grasping, but further considers both target exploration and singulation.

In comparison to target-agnostic grasping discussed above, target-oriented grasping has been much less explored, except for [17], [18], [4], [5]. In [4] object representations are learned via autonomous robot interaction with the environment for instance grasping. The work in [5] presents a multi-task domain adaptation framework to transfer the learned instance grasping policy from simulation to the real world. The environments in these works, however, tend to be sparse and thus the application scenarios are heavily limited. Moreover, visibility of the target is a strict precondition for representation computation or mask extraction to make these systems work as expected. In contrast, our method does not assume initial visibility of the target and take advantage of instance pushing to grasp the target instance in challenging clutter.

One work close to ours is visual pushing for grasping (VPG) by Zeng et al. [3], which proposes a Q-learning framework to learn complementary pushing and grasping policies for robot picking task with challenging arrangements. While VPG performs target-agnostic tasks and focuses on clearing the table, our approach instead learns a critic for target-oriented manipulations and propose subtask actors to solve a more general and complex problem, “grasping the invisible”. Furthermore, though it is possible to adapt VPG for target-oriented tasks by incorporating the target object mask, as

shown in the experiments in Sec. V-B, our approach which jointly trains a mask-informed critic and a classifier-based coordination actor is much more effective for grasping the target in clutter.

Another work [15] employs an instance pushing policy analogous to ours, in which a sole push policy is learned via Q-learning for the visible target in clutter. In contrast we utilize both pushing and grasping for the (visible or invisible) target and thus the application scenarios are enlarged. In [15] the singulation of the target is confirmed by a hand-crafted module checking the minimum distance from the nearest object, while we employ a neural network actor which learns to decide whether to push or grasp from self-experience. This implicit singulation scheme tends to improve the action efficiency since complete isolation is not necessary for a successful grasping in clutter, as shown in Fig. 3.

III. PROBLEM FORMULATION

The “grasping the invisible” problem we solve in this paper can be formulated as follows:

Definition 1. *Given a description (e.g., the class name) of the target object, the goal is to grasp the target which can be placed with arbitrary pose and occlusions in dense clutter via a finite sequence of pushes and grasps.*

Because of the pose variations and surrounding non-target objects, there are two challenging scenarios necessitating two subtasks

Subtask 1. *If the target instance is completely buried in clutter, then the robot searches for the target and breaks the structure to make it visible. We name this **exploration** task.*

Subtask 2. *Though clearly visible, the target instance might be closely surrounded by other objects, leaving no space for grasping. Thus sole instance grasping is impossible or inefficient without breaking the structured clutter by instance pushing. In the **coordination** task, the instance pushing and grasping need to be coordinated in a temporal manner so as to grasp the target with the most action efficiency.*

IV. METHOD

Inspired by [19], we propose an approach in an actor-critic format¹ to solve the problem, where the critic is learned for instance pushing and grasping through Q-learning, and the actors are proposed for the exploration and coordination subtasks from Q predictions by the critic and domain knowledge D , i.e., the policy is $\pi = f(Q, D)$.

A. Critic

In the Markov decision process, the robot performs an action a_t in state s_t , then transitions to state s_{t+1} , and receives the corresponding reward $R(s_t, a_t, s_{t+1})$. The goal of our critic is to learn an action-value function $Q_{\{p,g\}}^{\pi}(s, a)$

¹Here we borrow the name and format from the reinforcement learning literature.

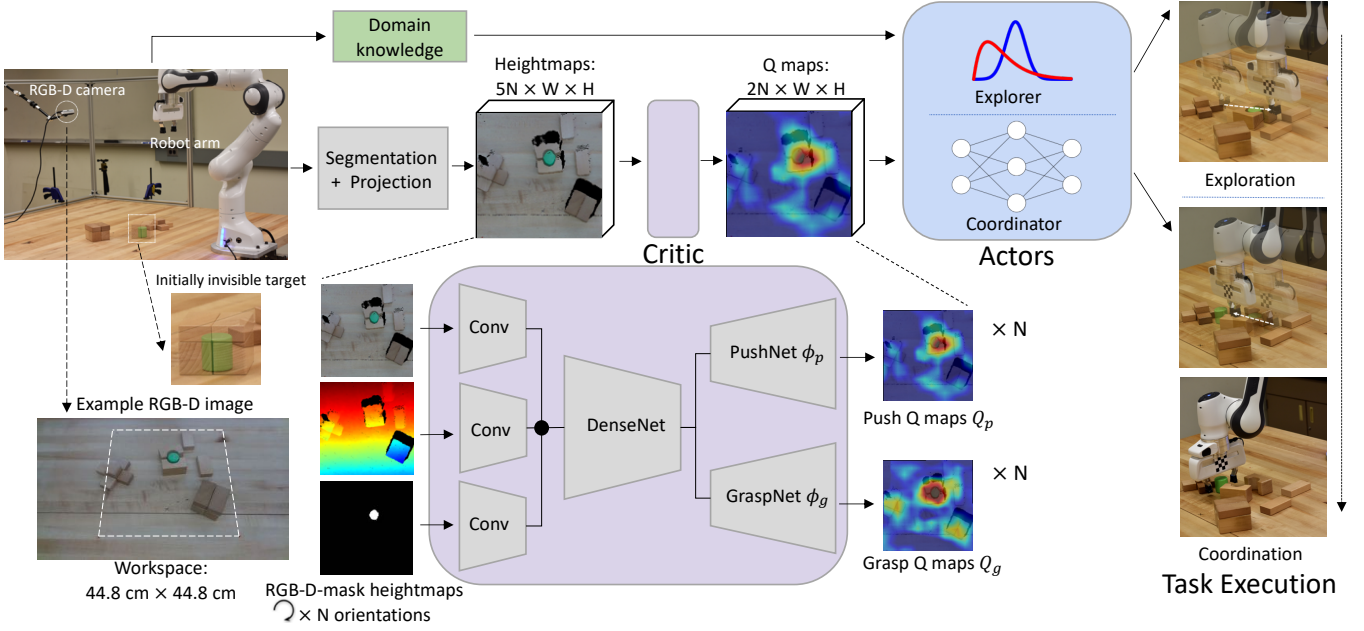


Fig. 2: **Overview.** The visual observations of the scene (an example image with the visible target is used for illustration purpose) together with the target mask from semantic segmentation are orthographically projected and then fed into the Q critic to output the pixel-wise push and grasp Q maps. The input heightmaps are rotated by N orientations to account for different pushing and grasping angles. The two actors, explorer and coordinator, take in the Q predictions and domain knowledge to execute the two subtasks.

which predicts the expected return for pushing or grasping action a in state s under a policy π .

As shown in Fig. 2, a fixed-mount RGB-D camera captures the predefined workspace. The RGB image is first passed into a pretrained semantic segmentation module to predict the target mask. The segmentation module robustly detects the target mask, even in heavy occlusions. See Appendix A for more details. Then RGB, depth and mask images are orthographically projected in the gravity direction with a known extrinsic parameter of the camera to construct color heightmap c_t , depth heightmap d_t and target mask heightmap m_t . We represent each state s_t as RGB-D-mask heightmaps of the scene at time t , i.e., $s_t = (c_t, d_t, m_t)$.

The critic is represented with a FCN in encoder-decoder architecture [20] to output pixel-wise Q maps. The RGB, depth and mask heightmaps are fed into the corresponding 2-layer residual [21] network for feature extraction and the output features are concatenated as the input to a DenseNet-121 [22] pretrained on ImageNet [23], to have the motion-agnostic features [24]. A push network ϕ_p and a grasp network ϕ_g take the features as input to predict push maps Q_p and grasp maps Q_g respectively. The networks ϕ_p and ϕ_g are with same architecture, a 3-layer residual network followed by bilinear upsampling.

Every pixel in the Q maps parameterizes a primitive pushing or grasping, so there is a direct mapping from Q maps to primitive motions. Every 2D pixel is mapped to the 3D action execution position through the depth heightmap. Different motion angles are achieved by rotating the input heightmaps by N orientations before feeding into the networks, and

there are N corresponding Q maps for pushing and grasping respectively [3]. We choose $N = 16$ in our system and the angle discretion is thus 22.5° .

B. Reward Shaping

Our reward scheme for the critic is divided into pre-action level and post-action level, and the maximum one is counted. For pre-action level, we check if the action is target-oriented. For post-action level, rewards are given if the desirable effects are achieved. The pre-action rewards are shaped to ease the pixel-wise Q learning, since the post-action rewards tend to be sparse.

An example of the reward scheme is given in Fig. 3. We assign $R_p(s_t, s_{t+1}) = 0.25$ if the intended pushing vector passes the mask m_t . Then $R_p(s_t, s_{t+1}) = 0.5$ is given for pushes that make more spaces around the target for future grasping. We dilate around m_t to construct the mask of the target border m_b (shown as the mask of light red color), and

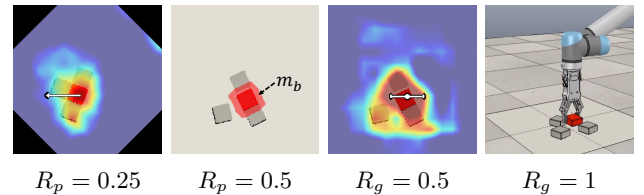


Fig. 3: **Example of our reward scheme.** One push and grasp are executed consecutively for the target (the red cylinder), and pre-action and post-action rewards corresponding to the actions are given.

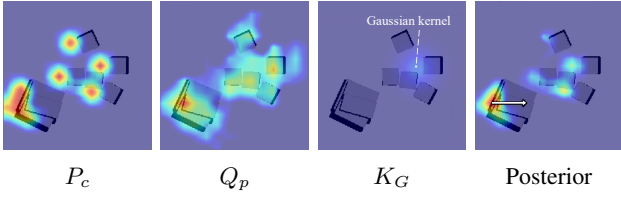


Fig. 4: **Example of exploration probability maps.** Clutter prior P_c , generic push maps Q_p and conditional Gaussian kernel K_G are multiplied to construct posterior probability maps, according to which the explorational pushing is executed. Only the map representing the intended pushing orientation is visualized here.

the space increase is detected if the border occupancy value o_b (defined as the number of pixels in m_b with height above the ground) decreased by some threshold. In the example, the pushing motion frees spaces around the target and thus the reward of 0.5 is given.

Similarly we assign $R_g(s_t, s_{t+1}) = 0.5$ for those grasps with intended grasping position in m_t and $R_g(s_t, s_{t+1}) = 1$ if the target is successfully grasped.

C. Actor

Exploration and coordination actors which take the outputs of the critic and domain knowledge as input are used to make the action decision in two subtasks.

Exploration actor. To effectively search for the target in the workspace, we propose a Bayesian-based explorer π_e . As shown in Fig. 4, we use the product of generic push maps Q_p and clutter prior P_c as the prior probability for searching. The constant all-ones mask [5], which represents all objects in the workspace as the potential target, is fed into ϕ_p to get a generic probability Q_p . P_c encodes the prior about edges of clutter along the intended pushing direction in the form of probability maps. These two constitute our prior for exploration. More details are delineated in Sec. V-A.

To avoid the robot getting stuck at some local area, we account for the past failing experience and construct a multimodal Gaussian kernel K_G with low peaks at the three most recent failed action locations. The kernel represents the conditional probability since every execution is conditional on the probability of last time. Every time an action is executed according to the location with maximum probability. The explorer is to execute the action based on the posterior probability maps

$$\pi_e = \arg \max_a K_G \circ (P_c \circ Q_p) \quad (1)$$

where \circ is the Hadamard product, also known as entrywise product.

Coordination actor. Different from the greedy deterministic policy used in VPG [3], we propose a classifier-based coordinator, denoted as π_c , to coordinate pushing and grasping. The binary classifier takes as input maximum push Q value $q_p = \max Q_p$, maximum grasp Q value $q_g = \max Q_g$, target border occupancy ratio $r_b = \frac{o_b}{\sum m_b}$, target

border occupancy norm $n_b = \frac{o_b}{\sum m_t}$ (o_b , m_b and m_t are the border occupancy value, the target border and the target mask discussed in Sec. IV-B) and the number of consecutive grasping failures c_g . Though q_p and q_g can somewhat reflect the chance of instance grasping, i.e., the larger difference might indicate higher chance of grasping, we also include the domain knowledge c_g , r_b and n_b as the input to the classifier. The reasons are 1) r_b and n_b are indicators of the clutteredness around the target but hard for the networks to learn directly and 2) we should encourage pushing if the robot keep grasping but failing.

Through iterations the program automatically labels the data as 1 if the target instance is grasped or 0 if the grasping position is within the mask m_t but results in a grasping failure (this might indicate dense clutter around the target). Thus the classifier is to predict the probability of successful instance grasping, and the motion type is selected according to the predicted probability and the action with maximum corresponding Q value is executed. We name the classifier as action classifier f_a (i.e., classify the state into push or grasp-favored) and the coordinator is formulated as

$$y = f_a(q_p, q_g, r_b, n_b, c_g)_{\{p, g\}} \quad (2)$$

$$\pi_c = \arg \max_a Q_y \quad (3)$$

where f_a is a function approximator composed of three fully connected layers with batch normalization [25] and ReLU [26]. It learns to signify the influential variables through its weights and drop unimportant factors by ReLU.

D. Training

The critic is trained by minimizing the temporal difference error δ_t as

$$\delta_t = Q(\theta_t; s_t, a_t) - (R_{a_t}(s_t, s_{t+1}) + \gamma \max_a Q(\theta_t^-; s_{t+1}, a)) \quad (4)$$

via the Huber loss

$$\mathcal{L}_\delta = \begin{cases} \frac{1}{2} \delta_t^2, & \text{if } |\delta_t| \leq 1 \\ |\delta_t| - \frac{1}{2}, & \text{otherwise} \end{cases} \quad (5)$$

where θ_t are the parameters of the critic network at time t and the target network parameters θ_t^- are held fixed between iterations. At time t , we pass gradients only through the single pixel on which the motion primitive was executed while all other pixels backpropagate with 0 loss. We train the critic with prioritized experience replay [27]. To deal with sparse rewards for instance grasping (especially at early stages), the hindsight experience replay technique [28] is used. If a non-target object is grasped at time t , we save the executed action a_t , the states, the mask of the grasped object m'_t and the posthoc labeled reward $R_{a_t}((c_t, d_t, m'_t), s_{t+1}) = 1$ for further experience replay training.

The coordinator is trained using the binary cross-entropy loss

$$\mathcal{L}_y = -(\bar{y} \log y + (1 - \bar{y}) \log(1 - y)) \quad (6)$$

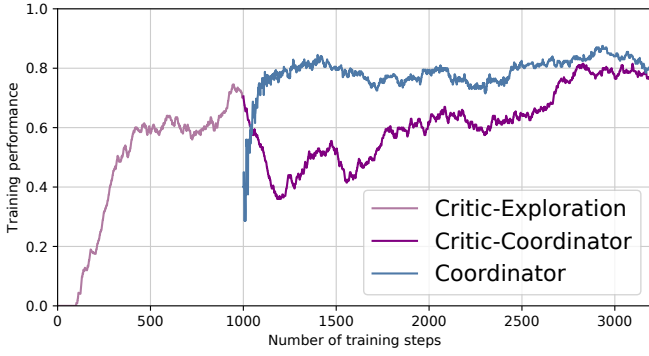


Fig. 5: **Training performance.** The purple lines indicate the instance grasping success rate of the Critic-Policy and the blue line indicates the training accuracy of the coordinator over training steps.

where y is the classifier predication and \bar{y} is the ground-truth label.

The actor-critic is trained with the following procedure: n target candidate instances (i.e., detectable by the semantic segmentation module) and m basic objects are randomly selected and dropped into the workspace in front of the robot and the robot needs to grasp one randomly appointed target. Once on a successful target grasping, the new target is appointed. The objects are again randomly dropped if the workspace is void of target candidates. Through iterations the robot automatically performs data collection for self-supervision.

Multi-stage learning is utilized in training our model. At the first stage we only train the critic in order to reach a good initialization, and the robot moves under the decayed ϵ -greedy policy π_ϵ . We set $m = 3$ to ease the learning for instance pushing or grasping. Then m increases to be 8 and the policy switches to be the randomly initialized coordinator π_c to learn coordinated decision making in structured dense clutter. In the mean time the critic is still under training and expected to accommodate π_c , i.e., fine-tuned from Q^{π_ϵ} to Q^{π_c} .

As shown in Fig. 5, only the critic is trained at the first stage (first 1000 iterations in our experiment) under π_ϵ exploration and reaches a high instance grasping success rate (defined as $\frac{\# \text{ successful instance grasping}}{\# \text{ total motions (pushes and grasps)}}$). Then we replace the policy to be the coordinator and start training the coordinator to gradually increase its prediction accuracy. Note that Critic-Coordinator finally achieves a higher instance grasping success rate in even more cluttered scenes.

We train our model on a machine with an NVIDIA GeForce GTX 1080 Ti GPU and an Intel i7-8700 CPU for 3k iterations (~ 8 hours).

E. Testing

Algorithm 1 explains the testing details of the Actor-Critic approach to grasping the invisible target. The algorithm is repeated over time until the robot grasps the target or exceeds the maximum number of motions. Each time one of the two actors are decided upon the existence of the target

Algorithm 1 Actor-Critic to grasping the invisible

Input: RGB-D image I

Output: action decision a_t at time t

```

1:  $M \leftarrow \text{ObjectSegmentation}(I)$ 
2: if  $M = \emptyset$  then  $\triangleright$  exploration subtask
3:    $M \leftarrow \text{AllOnesMask}()$ 
4:    $s_t \leftarrow \text{HeightmapProjection}(I, M)$ 
5:    $P_c \leftarrow \text{ClutterPrior}(s_t)$ 
6:    $Q_p \leftarrow \phi_p(s_t)$ 
7:    $K_G \leftarrow \text{GaussianKernel}(D)$ 
8:    $a_t \leftarrow \max_a K_G \circ (P_c \circ Q_p)$   $\triangleright$  explorer
9: else  $\triangleright$  coordination subtask
10:   $s_t \leftarrow \text{HeightmapProjection}(I, M)$ 
11:   $Q_p \leftarrow \phi_p(s_t), Q_g \leftarrow \phi_g(s_t)$ 
12:   $y \leftarrow f_a(\max_{\{p,g\}} Q_p, \max Q_g, D)$ 
13:   $a_t \leftarrow \max_a Q_y$   $\triangleright$  coordinator
14: end if

```

information, and the actor works by combining the critic Q predictions and the domain knowledge.

V. EXPERIMENTS

We train the system in simulation where all states are known. We executed a set of ablation studies for the exploration actor (explorer) and comparative experiments for the coordination actor (coordinator). The goal of the experiments are: 1) to show the importance of the extra domain knowledge in the actors, 2) to understand the limitation of each submodule in the explorer π_e and the advantages and robustness of π_e and 3) to demonstrate that our coordinator π_c can coordinate the instance pushing and grasping in structured clutter. The simulation environment and robot are kept the same with [3] for comparison purpose. We also run experiments on a real robot to show the performance of our system on “grasping the invisible” problem.

A. Exploration Subtask

To validate our approach, we run an ablation study for which our explorer is compared with the following methods in the exploration subtask:

Clutter-Prior builds the probability maps P_c for potential pushing actions based on the depth heightmap [29]. The heightmap is first translated along one fixed axis for 25 pixels (approximately twice the width of the closed gripper), then the pixel with enough depth difference between original and translated heightmap is recorded as 1 otherwise 0. This binary map is filtered with a 25×25 all-ones kernel to get a pixel-wise probability map. Like Q maps, the heightmap is also rotated by N orientations to construct N probability maps. P_c encodes prior about edges of clutter by detecting varying heights.

Generic-Push utilizes the generic pushing skills from ϕ_p taking in RGB-D heightmaps c_t, d_t and all-ones mask heightmap. Since it treats every single object indiscriminately, it lacks the sense of clutter.

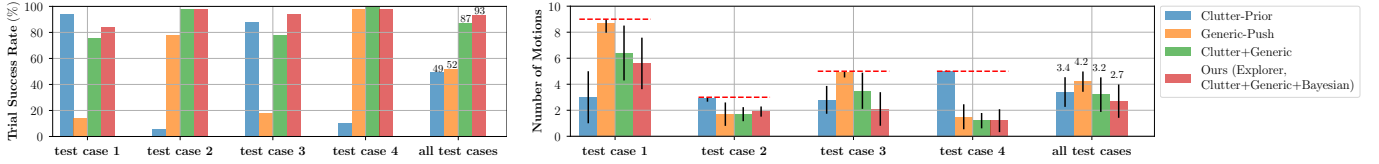


Fig. 6: **Performance in exploration subtask.** The task success rate (left) and the number of motions (right) of four approaches on the 4 test cases of complete occlusion. The plot clearly shows the effectiveness of our approach, **Explorer**, which achieves a task success rate of 93% with 2.7 motions in average. The red dotted line is the number limitation of motions.

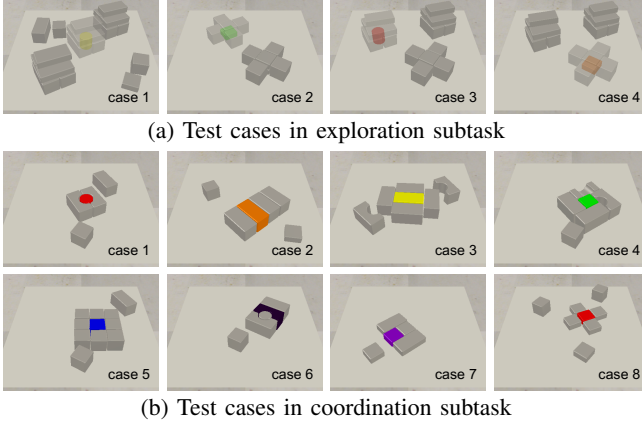


Fig. 7: **Test cases in simulation.** (a) shows 4 test cases in the exploration subtask, where the target is invisible and in (b) we show 8 challenging arrangements where the coordination between pushing and grasping is required. The target is the colored object.

Clutter+Generic is the Hadamard product of **Clutter-Prior** and **Generic-Push**, i.e., $P_c \odot Q_p$. By simply combining Q predictions and the domain knowledge, the robot balances between clutter prior and generic skills and achieves significant performance gain.

Clutter+Generic+Bayesian is the explorer in our system. It adds a Bayesian kernel K_G on **Clutter+Generic** to reduce the probability around the three most recent failed action locations, which improves the robustness of the system by avoiding getting stuck.

The test cases are shown in Fig. 7a. In each test case, the maximum number of pushes is $n_{\text{pushes}} = 2 * n_{\text{cluster}} - 1$ where n_{cluster} is the number of object clusters in the workspace. The robot is tasked to find the target via explorational pushes and allowed to stop if the target is found. We execute 50 runs on each test case and report the task success rate and the number of motions. Fig. 6 presents the performance of the above methods in the exploration subtask. Both **Clutter-Prior** and **Generic-Push** perform poorly in specific cases. For instance, **Clutter-Prior** is discouraging in either the equal height case (case 2) or the taller pyramid-like clutter case (case 4). **Generic-Push** is prone to push every object in the workspace in the test case 1 and 3, and hence it necessitates a large number of motions. By balancing between clutter prior and generic skills, **Clutter+Generic** works consistently well across all

TABLE I: Average Performance in the Exploration Subtask

| Method | Task Success Rate (%) | Number of Motions |
|-----------------|-----------------------|-----------------------------------|
| Clutter-Prior | 49.5 | 3.43 ± 1.14 |
| Generic-Push | 52 | 4.20 ± 0.78 |
| Clutter+Generic | 87.5 | 3.20 ± 1.33 |
| Our Explorer | 93.5 | 2.70 ± 1.28 |

test cases. Our explorer **Clutter+Generic+Bayesian** further improves the performance of **Clutter+Generic** in terms of the task success rate with the fewer number of motions. As shown in Table I, our explorer **Clutter+Generic+Bayesian** outperforms **Clutter+Generic** by 6% in terms of the task success rate and requires about 0.5 fewer average number of motions compared to **Clutter+Generic**.

B. Coordination Subtask

We compare the picking performance of our coordinator with the following baseline approaches:

RAND randomly chooses one of motion primitives and samples motion angle from the N angles and motion position in the target mask m_t .

Mask-VPG is an extension of VPG [3] by incorporating the mask m_t as post-processing. Given Q_p and Q_g maps for the indiscriminate task, we filter Q_p by a dilated target mask and Q_g by the target mask. The action with the highest Q value is executed.

Border-Heuristic is another extension of VPG by adding the mask as one input to the networks. The policy is ϵ -greedy and higher ϵ indicates higher pushing exploration rate. The base rate is $\epsilon_0 = 0.5$, and we adjust its value to accommodate maximum Q values q_p, q_g and the domain knowledge r_b, n_b, c_g defined in Sec. IV-C by a hard-coded heuristic. In brief ϵ is advanced with the decrease of $q_g - q_p$, the increase of r_b and n_b , and the growth of c_g . Note that the method takes the same input with our coordinator, but the difference is the subtask policy.

We evaluate the methods on 8 challenging test cases with adversarial structures shown in Fig. 7b. In each test case, the maximum number of motions is 5 and the robot is tasked to grasp the target in clutter. We execute 30 runs on each test case, and the task success rate and the number of motions are reported in Fig. 8. Our approach **Coordinator** clearly outperforms the other approaches in terms of both the task success rate and the number of motions. Overall **Coordinator** achieves 87.5% task success rate in the 8 challenging arrangements; **RAND** shows about

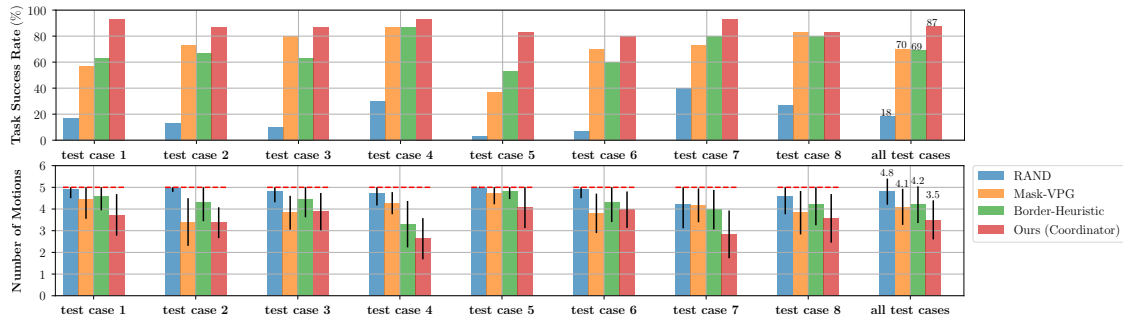


Fig. 8: **Performance in coordination subtask.** The task success rate (top) and the number of motions (bottom) of four approaches on the 8 test cases of challenging arrangements. The plot clearly shows the effectiveness of our approach, **Coordinator**, which achieves a task success rate of 87% with 3.3 motions in average.

TABLE II: Average Performance in the Coordination Subtask

| Method | Task Success Rate (%) | Number of Motions |
|------------------|-----------------------|-----------------------------------|
| RAND | 18.3 | 4.77 \pm 0.60 |
| Mask-VPG | 70.0 | 4.06 \pm 0.83 |
| Border-Heuristic | 69.2 | 4.25 \pm 0.85 |
| Our Coordinator | 87.5 | 3.51 \pm 0.90 |

18% chance of task success rate; the performance of **Mask-VPG** and **Border-Heuristic** are similar, while **Mask-VPG** shows slightly superior performance. **Mask-VPG** is originally designed for target-agnostic tasks, thus it lacks the reasoning about the target and surrounding objects. Though **Border-Heuristic** has exactly same input with **Coordinator**, the hard-coded heuristic limits the coordination of instance pushing and grasping. The comparison between **Border-Heuristic** and **Coordinator** shows the effectiveness of the actor for coordination. As shown in Table II, **Coordinator** increases by more than 17% in terms of the task success rate and requires about 0.6 fewer average number of motions compared with **Mask-VPG** and **Border-Heuristic**.

C. Real-robot Experiments

We evaluate our system on the “grasping the invisible” problem with a Franka EMIKA Panda robot using the model trained in simulation². Over 4 test cases as shown in Fig. 9, our approach and two baselines, **VPG** and **Mask-VPG**, are tested. Successful target grasping is manually checked for **VPG** as it is target-agnostic. When exploring **Mask-VPG** works as **VPG** (i.e., no mask post-processing) except that only pushing is enabled for fair comparison.

We run on each test case for 10 runs and the maximum number of motions for each run is 15. The robot is tasked to find the initially invisible target as well as grasp it in challenging clutter. Table III reports the task success rate and the number of total motions of three methods. Overall, our approach trained in simulation outperforms the domain-adapted baselines and achieves a task success rate of 85%, which shows our system is capable of generalizing to new environments, sets of objects of a similar shape to training

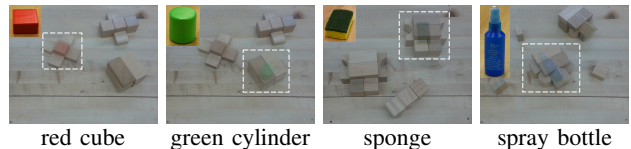


Fig. 9: **Test cases for real robot.** The invisible target is either a toy block or a novel object never seen in training.

TABLE III: Real-robot Results on “Grasping the Invisible”

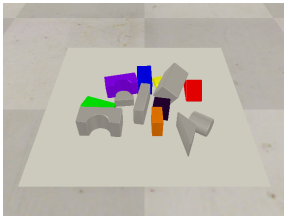
| Method | Task Success Rate (%) | Number of Total Motions |
|----------|-----------------------|-------------------------|
| VPG | 32.5 | 14.4 |
| Mask-VPG | 67.5 | 11.6 |
| Ours | 85.0 | 9.8 |

objects and adversarial arrangements. **VPG** shows a task success rate of only 32.5% with a high average number of motions. Target-agnostic **VPG** tends to prioritize grasping easily graspable objects while the invisible target is buried in heavy clutter. **Mask-VPG** is advanced by reducing the action field by the target mask, and its task success rate improves to be 67.5% with 11.6 average number of motions. In contrast to **Mask-VPG**, our approach outperforms by 17.5% in terms of the task success rate and requires about 1.8 fewer average number of motions. Through experiments we find that **Mask-VPG** tends to be less stable in real settings and the reasons are 1) it is not as robust as our approach with respect to noise when the mask is used as post-processing and 2) its policy lacks the capability of superior coordination that our approach demonstrates, and it tends to push a already well singulated target or make failed grasping in heavy clutter.

VI. CONCLUSIONS

In this work we presented the “grasping the invisible” problem and proposed a deep learning approach in an actor-critic format. The learning models of the approach were trained by self-supervision in simulation, and the system was evaluated in both simulated and real settings. Our actor-critic approach shows 93% and 87% task success rate on the two subtasks in simulation and 85% task success rate in the real robot experiments, which outperforms the other compared approaches by large margins. The evaluation results with the real robot show the generalization capability of our approach;

²We don’t fine-tune the model on the real robot though the idea how to collect data in the real world is available in [4]. For the comparison baselines, we use the available model trained in the real world [3].



Cluttered scenes



Segmentation results

Fig. 10: **Example of Semantic image segmentation.** The background is visualized in white color for best visualization.

the learned model in simulation was reliably transferred in the real setting and even generalizes to novel objects.

APPENDIX

A. Pretrained Perception Module

Semantic segmentation is widely used in 6D object pose estimation in cluttered scenes [30], [31], [32] and proves to be very robust to occlusions between objects. We choose Light-Weight RefineNet [33] as our perception module and pretrain it on the augmented data. Inspired by [31], we synthetically generated the training dataset covering all target candidate instances, rich pose variations of the objects and occlusions with a handful of labeled data. The pretrained model robustly segments the cluttered scenes, as shown in Fig 10.

REFERENCES

- [1] A. Eitel, N. Hauff, and W. Burgard, "Learning to singulate objects using a push proposal network," in *Proc. of the International Symposium on Robotics Research (ISRR)*, 2017.
- [2] C. Choi, W. Schwarting, J. DelPreto, and D. Rus, "Learning object grasping for soft robot hands," *IEEE Robotics and Automation Letters*, vol. 3, no. 3, pp. 2370–2377, 2018.
- [3] A. Zeng, S. Song, S. Welker, J. Lee, A. Rodriguez, and T. Funkhouser, "Learning synergies between pushing and grasping with self-supervised deep reinforcement learning," in *2018 IEEE/RSJ International Conference on Intelligent Robots and Systems (IROS)*. IEEE, 2018, pp. 4238–4245.
- [4] E. Jang, C. Devin, V. Vanhoucke, and S. Levine, "Grasp2vec: Learning object representations from self-supervised grasping," in *Conference on Robot Learning*, 2018, pp. 99–112.
- [5] K. Fang, Y. Bai, S. Hinterstoisser, S. Savarese, and M. Kalakrishnan, "Multi-task domain adaptation for deep learning of instance grasping from simulation," in *2018 IEEE International Conference on Robotics and Automation (ICRA)*. IEEE, 2018, pp. 3516–3523.
- [6] J. Bohg, A. Morales, T. Asfour, and D. Kragic, "Data-driven grasp synthesis: a survey," *IEEE Transactions on Robotics*, vol. 30, no. 2, pp. 289–309, 2013.
- [7] A. Sahbani, S. El-Khoury, and P. Bidaud, "An overview of 3d object grasp synthesis algorithms," *Robotics and Autonomous Systems*, vol. 60, no. 3, pp. 326–336, 2012.
- [8] J. Mahler, J. Liang, S. Niyaz, M. Laskey, R. Doan, X. Liu, J. A. Ojea, and K. Goldberg, "Dex-net 2.0: Deep learning to plan robust grasps with synthetic point clouds and analytic grasp metrics," *Robotics: Science and Systems (RSS)*, 2017.
- [9] D. Kalashnikov, A. Irpan, P. Pastor, J. Ibarz, A. Herzog, E. Jang, D. Quillen, E. Holly, M. Kalakrishnan, V. Vanhoucke, *et al.*, "Scalable deep reinforcement learning for vision-based robotic manipulation," in *Conference on Robot Learning*, 2018, pp. 651–673.
- [10] M. R. Dogar and S. S. Srinivasa, "A planning framework for non-prehensile manipulation under clutter and uncertainty," *Autonomous Robots*, vol. 33, no. 3, pp. 217–236, 2012.
- [11] A. Cosgun, T. Hermans, V. Emeli, and M. Stilman, "Push planning for object placement on cluttered table surfaces," in *2011 IEEE/RSJ international conference on intelligent robots and systems*. IEEE, 2011, pp. 4627–4632.
- [12] T. Hermans, J. M. Rehg, and A. Bobick, "Guided pushing for object singulation," in *2012 IEEE/RSJ International Conference on Intelligent Robots and Systems*. IEEE, 2012, pp. 4783–4790.
- [13] L. Chang, J. R. Smith, and D. Fox, "Interactive singulation of objects from a pile," in *2012 IEEE International Conference on Robotics and Automation*. IEEE, 2012, pp. 3875–3882.
- [14] M. Danielczuk, J. Mahler, C. Correa, and K. Goldberg, "Linear push policies to increase grasp access for robot bin picking," in *2018 IEEE 14th International Conference on Automation Science and Engineering (CASE)*. IEEE, 2018, pp. 1249–1256.
- [15] K. Marios and M. Sotiris, "Robust object grasping in clutter via singulation," in *2019 International Conference on Robotics and Automation (ICRA)*. IEEE, 2019, pp. 1596–1600.
- [16] A. Boularias, J. A. Bagnell, and A. Stentz, "Learning to manipulate unknown objects in clutter by reinforcement," in *Twenty-Ninth AAAI Conference on Artificial Intelligence*, 2015.
- [17] L. Pinto and A. Gupta, "Supersizing self-supervision: Learning to grasp from 50k tries and 700 robot hours," in *2016 IEEE international conference on robotics and automation (ICRA)*. IEEE, 2016, pp. 3406–3413.
- [18] E. Jang, S. Vijayanarasimhan, P. Pastor, J. Ibarz, and S. Levine, "End-to-end learning of semantic grasping," in *Conference on Robot Learning*, 2017, pp. 119–132.
- [19] V. Mnih, A. P. Badia, M. Mirza, A. Graves, T. Lillicrap, T. Harley, D. Silver, and K. Kavukcuoglu, "Asynchronous methods for deep reinforcement learning," in *International conference on machine learning*, 2016, pp. 1928–1937.
- [20] V. Badrinarayanan, A. Kendall, and R. Cipolla, "Segnet: A deep convolutional encoder-decoder architecture for image segmentation," *IEEE transactions on pattern analysis and machine intelligence*, vol. 39, no. 12, pp. 2481–2495, 2017.
- [21] K. He, X. Zhang, S. Ren, and J. Sun, "Deep residual learning for image recognition," in *Proceedings of the IEEE conference on computer vision and pattern recognition*, 2016, pp. 770–778.
- [22] G. Huang, Z. Liu, L. Van Der Maaten, and K. Q. Weinberger, "Densely connected convolutional networks," in *Proceedings of the IEEE conference on computer vision and pattern recognition*, 2017, pp. 4700–4708.
- [23] J. Deng, W. Dong, R. Socher, L.-J. Li, K. Li, and L. Fei-Fei, "Imagenet: A large-scale hierarchical image database," in *2009 IEEE conference on computer vision and pattern recognition*. IEEE, 2009, pp. 248–255.
- [24] L. Pinto and A. Gupta, "Learning to push by grasping: Using multiple tasks for effective learning," in *2017 IEEE International Conference on Robotics and Automation (ICRA)*. IEEE, 2017, pp. 2161–2168.
- [25] S. Ioffe and C. Szegedy, "Batch normalization: Accelerating deep network training by reducing internal covariate shift," in *International Conference on Machine Learning*, 2015, pp. 448–456.
- [26] V. Nair and G. E. Hinton, "Rectified linear units improve restricted boltzmann machines," in *Proceedings of the 27th international conference on machine learning (ICML-10)*, 2010, pp. 807–814.
- [27] T. Schaul, J. Quan, I. Antonoglou, and D. Silver, "Prioritized experience replay," *arXiv preprint arXiv:1511.05952*, 2015.
- [28] M. Andrychowicz, F. Wolski, A. Ray, J. Schneider, R. Fong, P. Welinder, B. McGrew, J. Tobin, O. P. Abbeel, and W. Zaremba, "Hindsight experience replay," in *Advances in Neural Information Processing Systems*, 2017, pp. 5048–5058.
- [29] A. Zeng, "visual-pushing-grasping," 2018. [Online]. Available: <https://github.com/andyzeng/visual-pushing-grasping>
- [30] Y. Xiang, T. Schmidt, V. Narayanan, and D. Fox, "Posecnn: A convolutional neural network for 6d object pose estimation in cluttered scenes," *Robotics: Science and Systems (RSS)*, 2018.
- [31] A. S. Periyasamy, M. Schwarz, and S. Behnke, "Robust 6d object pose estimation in cluttered scenes using semantic segmentation and pose regression networks," in *2018 IEEE/RSJ International Conference on Intelligent Robots and Systems (IROS)*. IEEE, 2018, pp. 6660–6666.
- [32] C. Wang, D. Xu, Y. Zhu, R. Martín-Martín, C. Lu, L. Fei-Fei, and S. Savarese, "Densefusion: 6d object pose estimation by iterative dense fusion," in *Proceedings of the IEEE Conference on Computer Vision and Pattern Recognition*, 2019, pp. 3343–3352.
- [33] V. Nekrasov, C. Shen, and I. Reid, "Light-weight refinenet for real-time semantic segmentation," *arXiv preprint arXiv:1810.03272*, 2018.